



Available online at www.sciencedirect.com

ScienceDirect

www.elsevier.com/locate/jes

JES
JOURNAL OF
ENVIRONMENTAL
SCIENCES
www.jesc.ac.cn

Simultaneous measurement of aqueous redox-sensitive elements and their species across the soil-water interface

Zhao-Feng Yuan^{1,2,3}, Williamson Gustave^{1,2,4}, Raju Sekar⁵, Jonathan Bridge⁶, Jia-Yue Wang¹, Wei-Jia Feng¹, Bin Guo^{7,*}, Zheng Chen^{1,*}

¹ Department of Health and Environmental Sciences, Xi'an Jiaotong-Liverpool University, Jiangsu 215123, China

² Department of Environmental Science, University of Liverpool, Liverpool L69 7ZX, UK

³ Department of Plant Science, Tarim University, Xinjiang 843300, China

⁴ Chemistry, Environmental & Life Sciences, University of The Bahamas, Nassau, Bahamas

⁵ Department of Biological Sciences, Xi'an Jiaotong-Liverpool University, Jiangsu 215123, China

⁶ Department of Natural and Built Environment, Sheffield Hallam University, Sheffield S1 1WB, UK

⁷ Institute of Environment, Resource, Soil and Fertilizer, Zhejiang Academy of Agricultural Sciences, Zhejiang 310021, China

ARTICLE INFO

Article history:

Received 31 July 2020

Revised 6 September 2020

Accepted 6 September 2020

Available online 25 September 2020

Keywords:

Porewater

Soil-water interface

Arsenic

Iron

Sulfur

Species

ABSTRACT

The redox-sensitive elements, such as iron, manganese, sulfur, phosphorus, and arsenic, shift their speciation every millimeter (mm) across the soil-water interface in the flooded soil environments. Monitoring of element speciation at this high-resolution (HR) within the SWI is still difficult. The key challenge lies in obtaining sufficient porewater samples at specific locations along the soil gradient for downstream analysis. Here with an optimized inductively coupled plasma mass spectrometry (ICP-MS) method and a HR porewater sampler, we demonstrate mm-scale element profiles mapping across the SWI in paddy soils. High-concentrations of iron and manganese (> 10 mg/L) were measured by ICP-MS in an extended dynamic range mode to avoid signal overflow. The iron profile along the SWI generated by the ICP-MS method showed no significant difference ($p < 0.05$) compared to that measured independently using a colorimetric method. Furthermore, four arsenic (arsenite, arsenate, monomethylarsonic and dimethylarsinic acid), two phosphorus (phosphite and phosphate) and two sulfur (sulfide and sulfate) species were separated in 10 min by ion chromatography -ICP-MS with the NH_4HCO_3 mobile phase. We verified the technique using paddy soils collected from the field, and present the mm-scale profiles of iron, manganese, and arsenic, phosphorus, sulfur species (relative standard deviation < 8%). The technique developed in this study will significantly promote the measurement throughput in limited samples (e.g. 100 μL) collected by HR samplers, which would greatly facilitate redox-sensitive elements biogeochemical cycling in saturated soils.

© 2020 The Research Center for Eco-Environmental Sciences, Chinese Academy of Sciences. Published by Elsevier B.V.

* Corresponding authors.

E-mails: ndgb@163.com (B. Guo), Zheng.Chen@xjtu.edu.cn (Z. Chen).

Introduction

In flooded soils, the chemical environments of the surface water and saturated sediment porewater are very different. The surface water is oxidizing due to the high dissolved O₂, however, the sediments are generally reducing owing to the lack of O₂ and the abundance of organic matter (Frenzel et al., 1992). The O₂ can only penetrate the upper sediment to a depth of a few millimeters (mm) (Ratering and Schnell, 2001). As a result, the narrow boundary zone between the surface water and sediments, i.e. soil-water interface (SWI), displays a sharp redox decrease with depth (Huo et al., 2015; Jones et al., 2018). Iron (Fe), manganese (Mn), and sulfur (S) are the most important elements in SWI, existing in both solid and dissolved phases through complex redox reactions (Peng et al., 2019). The redox processes of Fe, Mn, and S significantly impact the fate of many elements of environmental and agricultural concern, such as arsenic (As) and phosphorus (P) (Gao et al., 2016, 2006; McAdams et al., 2016; Pi et al., 2018). Although it is of great importance to study the behavior of these elements in SWI, the high-resolution (HR) mm-scale mapping of those elements and their species has been severely limited to date by the lack of suitable available methods.

Many efforts have been made to measure the mm-scale element profile in porewater along SWI. The diffusive gradient in thin films technique (DGT) is one of the best, which can even depict the elements' pattern in μm scale, however it measures the flux instead of the equilibrated concentration (Davison and Zhang, 1994; Fang et al., 2018; Yin et al., 2020). The equilibrated concentrations can be measured by the diffusive equilibrium in thin films (DET) technique and in situ equilibrium dialysis samplers (peeper) (Arsic et al., 2018; Bottrell et al., 2007; Di et al., 2012; Dočekalová et al., 2002; Guan et al., 2015; Monbet et al., 2008). The DET probe resolution is 2 mm when using the strip-cutting method (Dočekalová et al., 2002; Gao et al., 2007), and can reach 1 mm when combining reagent dying and computer imaging densitometry detection (Bennett et al., 2012b; Robertson et al., 2008). Peepers have relatively low spatial resolution (~ 5 mm) compared to DET because handling the water in peeper chambers is not as convenient as the gels in DET probe (Di et al., 2012; Wen et al., 2019). Recently, we developed a novel porewater sampler, called *In-situ* Porewater Iterative (IPI) sampler, to monitor the mm-scale heterogeneity of trace metals in saturated soils (Yuan et al., 2019). The IPI sampler has a comparable HR (~ 2 mm) as DET probe. Unlike DET and peeper, the IPI sampler can be used repeatedly at a certain place without need for removal or destructive sampling. Another advantage of IPI samplers is to obtain clean liquid porewater sample directly, which is almost ready for downstream instrumental analysis. Due to these advantages, the IPI sampler was very suited for mm-scale element profile mapping.

Simultaneous measurement of multi-element profiles at HR across SWI presents significant additional challenges. The sharp and sensitive redox gradient along SWI requires that the porewater volume sampled should be as small as possible to minimize the disturbance to the sampling environment (Seeberg-Elverfeldt et al., 2005), and yet large enough to meet the minimum sample size for sensitivity and specificity

analysis of all the interested parameters (Arsic et al., 2018; Bennett et al., 2012a; Ding et al., 2016; Motelica-Heino et al., 2003). The HR samplers (e.g. DET, HR peeper, IPI samplers) designed for element profile mapping generally can only take less than 0.5 mL solution (Yuan et al., 2019), which is a bare minimum for one sample injection with most analytical techniques, like inductively coupled plasma mass spectrometry (ICP-MS) (Xu et al., 2017), ICP-optical emission spectrometry (Cheng et al., 2012), colorimetric method (Lumbaque et al., 2019). An alternative to collect more samples is to collect porewater repeatedly at different places or times, assuming the soil or sediment matrix is homogenous and stable over time. However, this assumption is severely limiting and constrains the ability to probe the heterogeneity and dynamics of SWI biogeochemistry as a function of location and in response to changing environmental conditions (Arsic et al., 2018; Yuan et al., 2019). Thus, it would be better to solve the issue by optimizing the analytical techniques used in extracting data from the samples.

ICP-MS has been widely applied to understand the element behaviors in various environments due to its broad spectrum and very low detection limits (Cotta and Enzweiler, 2009). Studies of rhizospheric element profiles have greatly benefited from developments in ICP-MS technologies. For example, the combination of laser ablation (LA)-ICP-MS with DGT allows mapping of μm -scale element fluxes and provided key information for understanding As behaviors on the root apexes (Williams et al., 2014). More recently, a new approach, called extended dynamic range (EDR), was introduced to simultaneously measure major and trace metals by ICP-MS (Hilbig et al., 2017). The EDR mode can attenuate the counts of selected elements through the spectrometer by tuning the 'rejection parameter a' (Rpa), thus it enables the detection of major and minor elements in a single run (Hilbig et al., 2017). EDR mode is potentially ideal to measure multi-element concentrations in volume-limited samples, such as the porewater sampled by HR samplers, which contains Fe and Mn over 10 mg/L, and other traces at $\mu\text{g}/\text{L}$ concentrations. However, the combination of HR samplers and ICP-MS under EDR mode has not been tested to date.

The small porewater sample volume also hinders the measurement of element speciation. Arsenic, P and S species play crucial roles in aquatic biogeochemical cycling (Chen et al., 2019; Sun et al., 2017). Traditionally, phosphate, P(V), is measured by colorimetric method (molybdate blue) (Rietra et al., 2001), sulfide, S(-II), by micro-electrode and spectrophotometric method (Laskov et al., 2007), sulfate, S(VI), by ion chromatography (IC) (Keller-Lehmann et al., 2006), arsenite and arsenate, As(III,V), by IC-ICP-MS (Gallagher et al., 2001). Summing up, to measure all these analytes in a single sample by standard methodologies, it requires an aliquot volume of several mL, far more than the porewater volume collected from HR samplers (Xu et al., 2012; Yuan et al., 2019). Among methods noted here, IC-ICP-MS can measure all the species, but is limited to the appropriate mobile phase. A review of the literature (Chen et al., 2019; McDowell et al., 2004; Morton et al., 2005; Reid et al., 2020; Suzuki et al., 2009) revealed that NH₄HCO₃ mobile phase, which is free of As, P, and S, can separate P, S and As species. Combined with the ICP-MS method (Hilbig et al., 2017), use of NH₄HCO₃ elution IC-ICP-

MS thus presents the possibility of accurate and rapid quantification of key major and minor element concentration and speciation within SWI profiles from small samples obtained by HR samplers such as IPI (Yuan et al., 2019), enabling non-destructive, mm-scale and repeated probing of SWI chemistry over time and therefore overcoming several key limitations of existing approaches outlined above.

This study demonstrates simultaneous measurement of multi-element and multi-species concentration profiles in flooded soil porewater using a HR sampler (IPI, after Yuan et al. (2019)) combined with the optimized ICP-MS and IC-ICP-MS method. The typical redox-active elements found in soil porewater, including Fe, Mn, As, P and S, and the common species of As, P, and S, including phosphite (P(III)), P(V) , S(-II) , S(VI) , monomethylarsonic acid (MMA), dimethylarsinic acid (DMA), As(III) , As(V) , were investigated in flooded paddy soils. This study directly addresses the challenge of maximizing the chemical information obtainable from increasingly small sample volumes, which would greatly enhance the measurement range, throughput and application potential of HR samplers.

1. Materials and methods

1.1. Reagents and materials

All reagents used in this study were of analytical grade or higher, and purchased from Aladdin Chemical Reagent Co., Ltd. (Shanghai, China), unless stated otherwise. Element standards for calibration, including As, Fe, Mn, P, S as well as P, S, and As species, were supplied by Guobiao (Beijing) Testing & Certification Co., Ltd. (Beijing, China). All solutions were prepared with ultrapure water (18.2 MΩ cm, Millipore Corp., Bedford, USA) deoxygenated by bubbling pure N_2 overnight.

Before the soil was sampled from paddy fields in Shaoguan (SG, 25°6'N, 113°38'E), obvious stones and plant debris were mechanically removed by shovels. In total, ~50 kg soils from the top layer (0–20 cm) were collected. The soils were directly transported to the laboratory, and homogenized by passing through a 1.0 mm diameter wet sieve. The soil characteristics are shown in Appendix A Table S1.

1.2. Porewater sampler preparation

The IPI sampler used in this study has a similar design as described in detail in our previous study (Yuan et al., 2019), with some minor modifications noted here. A novel hollow fiber membrane tube (modified polyethersulfone, 20 nm pore size, inner × outer diameter × length = 1.0 mm × 1.7 mm × 35 mm, 27.5 μL , Motimo Membrane Technology Co., Ltd., Tianjin, China) and two pipes (PTFE, inner × outer diameter × length = 0.5 mm × 1.0 mm × 180 mm, 35 μL) were used to construct the IPI sampler. The pore size of the membrane was demonstrated (Appendix A Fig. S1) with scanning electron microscopy (SEM) JSM-7600 (JEOL Ltd., Japan). The updated membrane does not contain fluoride or other potential chelators, which can avoid the complexation of the membrane for certain analytes (e.g. lead) (Yuan et al., 2019).

When the IPI sampler is deployed into solution or saturated soils, solutes around the hollow fiber membrane tube can diffuse through the membrane (Appendix A Fig. S2A). The solution inside the tube is pumped out and collected when the diffusion reaches equilibrium (Appendix A Fig. S2B). During the deployment, silicon caps are applied to seal the IPI sampler to avoid potential contamination (e.g. gasoline) from the atmosphere. During each sampling event, 27.5 μL liquid sample in the sampling tube is mixed with 70 μL ultrapure water in pipes when they are pumped out from the sampler. This indicates ~100 μL porewater sample can be sampled each time by the IPI sampler, with a dilution factor of 3.5.

Thirty-four IPI samplers were horizontally assembled side by side in a 3D printed holder (cavity cuboid, length × width × height = 40 mm × 30 mm × 120 mm, Appendix A Fig. S2C-E). The IPI sampler array, i.e. SWI profiler, can sample the porewater every 1.7 mm along SWI (Appendix A Fig. S2C). The SWI profiler has a sampling depth of 60 mm and was stored in O_2 -free ultrapure water before deploying into flooded soils (Appendix A Fig. S2F), following the procedure described in Yuan et al. (2019).

1.3. Analytical method and quality control

Element concentrations were quantified by ICP-MS (NexION 350X, PerkinElmer, Inc., Shelton, CT USA). The conditions were as follows: EDR mode; dynamic reaction cell (DRC) mode (O_2 , gas flow, 1.0 mL/min); data only analysis; RF power 1600 W; plasma gas flow rate 15 L/min; auxiliary gas flow 1.2 L/min; nebulized gas flow 0.94 L/min; nickel sampling and skimmer cones. The Rpa in EDR mode is a voltage parameter, which can tune bandpass of m/z that has stable trajectories (Tanner and Baranov, 1999). This parameter functions for the precursors of target analyte generated from dynamic reaction/collision cell. When $\text{Rpa} = 0$ (default value), a wide range bandpass of m/z is obtained, while non-zero Rpa (0–0.24) creates a narrow bandpass of m/z . The sensitivity of m/z is proportional to the width of bandpass, hence the upregulation of Rpa provides an option to suppress the high sensitivity of m/z caused by high abundance analyte or potential interferences. When using Rpa under different analytical modes, the Rpa value can be manually set for the interested element.

The porewater sample collected by the IPI sampler was introduced into ICP-MS by a PFA-200 Microflow Nebulizer (0.2 mL/min uptake rate). Iron, Mn As, P and S were measured by ICP-MS in EDR and DRC mode. Counts of $^{91}\text{AsO}^+$, $^{57}\text{Fe}^+$, $^{47}\text{PO}^+$, $^{48}\text{SO}^+$ and $^{55}\text{Mn}^+$ were recorded.

Element species were measured by IC-ICP-MS. The IC (Dionex ICS-1100, Thermo Scientific, USA) consisted of a standard 25 μL sample loop and an anion-exchange column (Ion-Pac AS23, 250 mm × 4 mm, Dionex). Mobile phases used for the separation were 20 mmol/L NH_4HCO_3 at pH 10.7 (Suzuki et al., 2009), with a flow rate of 1.0 mL/min. The analytical column was connected to a Type C0.5 Glass Nebulizer of the ICP-MS. The standards were prepared in neutral conditions (pH 7; 100 $\mu\text{g/L}$ P(III) , P(V) , As(III) , As(V) , MMA and DMA; 1 mg/L S(-II) and S(VI)).

When developing the calibration curve, a series of standard solutions, containing 1.0/10/100, 2.0/20/200, 5.0/50/500, 10/100/1000, 20/200/2000 $\mu\text{g/L}$ As&Mn/P/Fe&S in 2% HNO_3 ,

were measured ($n = 3$). For As, P and S species, a series of standard solutions, containing 0/0/0, 1.0/20/500, 2.0/50/1000, 5.0/100/2000, 10/200/5000 $\mu\text{g/L}$ DMA/P(V)/S(VI) under pH 7, were measured. Peak area was used to fit the standard curve, and three times standard deviation was used to calculate the limit of detection (LOD). Data quality was assured by testing a spiked standard after every 30 samples.

1.4. The sampling of total elements and element species by IPI samplers

Total elements were prepared in acidic conditions (pH 2; 10 $\mu\text{g/L}$ As and Mn; 10 mg/L Fe, P, and S), and As species were prepared in neutral conditions (pH 7; 100 $\mu\text{g/L}$ As(III), As(V), MMA and DMA). Those solutions were made by diluting the relative standards with ultrapure water. To determine the equilibrium time required for IPI samplers to sample Fe, Mn, As, P, S as well as As species, the time-dependent response of the sampler to those solutes was investigated in solutions. The samples inside the samplers were measured after 0, 0.5, 1, 3, 6, and 12 hr equilibrium time by ICP-MS or IC-ICP-MS.

1.5. Multi-element profile mapping

To detect the element profile, the SWI profilers were inserted into flooded soils in a pot (diameter \times height = 12 cm \times 20 cm), with 10 mm above SWI and 50 mm in soils (Appendix A Fig. S2C). Two replicates were conducted.

The paddy pot soils were filled with ultrapure water with ~3 cm overlying water, and the water depth was maintained daily by supplementing ultrapure water during the experiment. The soils were allowed to stabilize (22 °C, dark conditions) for three months before the deployment of SWI profilers. Before sampling, the solution inside IPI samplers was replaced by O₂-free ultrapure water driven by an injection pump (TYD01, Lei Fu, China) (Appendix A Fig. S3), with a velocity of 1.0 mL/min.

Based on the equilibrium test of analytes in this study, the sampling interval was set as 24 h. The sampled solution was preserved in the O₂-free EDTA solution (Gallagher et al., 2001). The EDTA solution (2 g/L) was online mixed with the porewater in a 1:3 vol. ratio driven by two injection pumps (Appendix A Fig. S3), with a velocity of 0.25 and 0.75 mL/min respectively. The mixed sample was carefully collected in a clean 0.6 mL centrifuge tube. In total, ~100 μL porewater was collected with an EDTA concentration of 500 mg/L. Each sample was divided into two parts (~50 μL per part) and measured by ICP-MS and IC-ICP-MS respectively. Additionally, a microplate reader was used to measure the Fe profile in paddy soil with the 1, 10-phenanthroline method ($\lambda = 510$ nm) (Lumbaque et al., 2019). Before measurement, the O₂-free colorimetric reagent was online mixed with the porewater sample in a 1:1 vol. ratio driven by two injection pumps (Appendix A Fig. S3), and ~200 μL solution was collected and transferred into 96-well plate (200 μL) for absorbance determination in a microplate reader (Tecan-Spark, Tecan Trading AG, Zurich, Switzerland). Finally, mm-scale profiles of multi-element and multi-species were mapped and evaluated.

1.6. Data analysis

R software (version 3.5.0) was used to analyze and plot the data in this study. We used the standard deviation to show the variance of the data. Data of different methods were subjected to one-way analysis of variance (ANOVA) to determine statistical significance ($p < 0.05$) using SPSS 22 software (SPSS Inc., Chicago, USA).

2. Results and discussion

2.1. The time-dependent sampling efficiencies of Fe, Mn, As, P and S by IPI samplers

Initially, the trans-membrane diffusion of Fe, Mn, As, P, and S in solution condition was studied. This was done to determine the applicability of IPI samplers in collecting solutions with those elements, which is a prerequisite before using the sampler to collect those elements in soil porewater. Significant peaks of all the five elements were observed with a 50 μL solution (Appendix A Fig. S4). The equilibration test showed the concentrations of those elements increased rapidly in the first three hour, and then reached a plateau representing their concentration in solutions (Appendix A Fig. S5). The time-dependent curves were consistent with our previous report for As, antimony, cadmium, lead, and nickel (Yuan et al., 2019). Considering the presence of dissolved organic matters, which could slow down the diffusion of solutes (Dočekalová et al., 2002; Reynolds et al., 2004; Yuan et al., 2019; Zhai et al., 2018), we deployed the IPI sampler at 24 hr equilibration period in saturated soils.

2.2. The effect of Rpa value on Fe and Mn detection

The Fe and Mn signals can be attenuated via tuning the Rpa value in ICP-MS (Hilbig et al., 2017). The response of Fe and Mn signals to Rpa from 0 to 0.02 is shown in Appendix A Fig. S6. The results indicated that Fe and Mn counts were very sensitive to Rpa value in a range from 0.0035 to 0.0084, in which Fe counts decreased linearly from 300,000 to 25,000, and Mn from 85,000,000 to 1,000,000.

Furthermore, the LODs of Fe and Mn are 21.2, 30.9, 210 and 0.504, 1.53, 1.56 $\mu\text{g/L}$ under Rpa 0, 0.005, and 0.01 respectively. Although LODs for Fe and Mn values decreased when the Rpa increased from 0 to 0.01, however it was sufficient for the Fe and Mn detection, since their concentrations are often found above 1 mg/L in field porewaters (Gustave et al., 2018b; Wang et al., 2019; Xu et al., 2017). When the ICP-MS was used to measure major elements (e.g. Fe) in low abundance, high Rpa may lead to the unsuccessful determination due to the relatively low LOD, thus is not recommended.

2.3. Comparison of colorimetric and ICP-MS for measuring Fe profiles in field samples

The ICP-MS application on Fe and Mn measurement was further investigated with paddy soil samples. With the method, simultaneous measurement of Fe, Mn, As, P, and S was

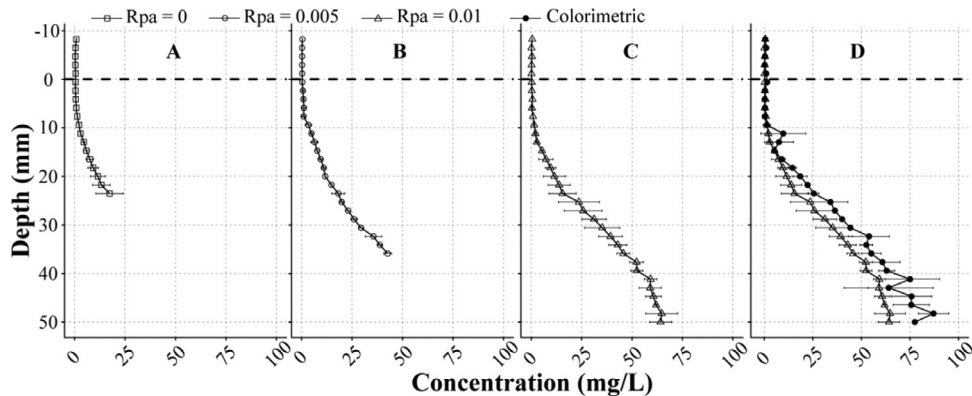


Fig. 1 – Iron profiles measured by ICP-MS under extended dynamic range mode or colorimetric method (phenanthroline) in Shaoguan (SG) paddy. (A-C): Fe profile measurement with ICP-MS method when ‘rejection parameter a’ (Rpa) = 0, 0.005 and 0.01 respectively; (D) Fe profile measured by colorimetric and ICP-MS method (Rpa = 0.01). The triangle symbols in (C) and (D) share the same dataset. The error bar is the standard deviation ($n = 2$). The black dashed line at depth zero is the soil-water interface.

achieved in the paddy soil samples. The determination coefficients for all the five elements were > 0.99 (Appendix A Fig. S7). The LODs for As, P and S were 0.490, 7.76, and $60.2 \mu\text{g/L}$, respectively, which agrees well with previous reports where As, P and S were measured with the ICP-MS (Persson et al., 2009; Yuan et al., 2019). Most studies on porewater Fe used colorimetric analysis for Fe quantification (Arsic et al., 2018; Bennett et al., 2012b). To compare our method with the colorimetric method, two porewater samples were measured using each method.

The Fe profile measured by the ICP-MS with different Rpa values is shown in Fig. 1. ICP-MS method with Rpa 0 was unable to measure Fe in soil depth > 25 mm when $\text{Fe} > 17 \text{ mg/L}$ in soil porewater because of signal overflow (Fig. 1A). Increasing the Rpa from 0 to 0.005 extended the Fe measurement along soil depth from ~ 25 mm to ~ 36 mm (Fig. 1A and B), however Rpa 0.005 was still unable to avoid the detector saturation of $\text{Fe} > 42 \text{ mg/L}$ in deep soil porewaters (Fig. 1B). Fig. 1C shows Fe profile could only be measured after the Rpa value was adjusted to 0.01 with $\text{Fe} \leq 70 \text{ mg/L}$. Similarly to Fe, Rpa 0.005 or 0.01 allowed Mn measurement when $\text{Mn} \leq 3.8 \text{ mg/L}$ in soil porewaters (Appendix A Fig. S9). Although the upper limit was altered with different Rpa values, the Fe and Mn profiles were identical in top soils (0 - 25 mm) (Fig. 1A-C, Appendix A Fig. S9).

The porewater samples collected from the same location were also measured by the colorimetric method (Fig. 1D). Both colorimetric and ICP-MS methods gave similar results of Fe profiles ($p > 0.05$). However, Fe concentration measured by the colorimetric method was slightly higher than that obtained by the ICP-MS method. The higher Fe values obtained by the colorimetric method could be attributed to the interference from other cations (e.g. Mn, calcium, zinc) in the porewater (Hatat-Fraile and Barbeau, 2019; Miranda et al., 2016). Therefore, Fe concentrations might have been overestimated as was reported in previous studies (Braunschweig et al., 2012; Miranda et al., 2016).

2.4. Profiling of total As, Fe, Mn, P and S across SWI

Using the ICP-MS coupled with IPI samplers, we were able to simultaneously measure Fe, Mn, As, P, and S at the mm-scale co-distributions of those elements (Fig. 2, relative standard deviation $< 8\%$). As shown in Fig. 2, the Fe remained at low concentrations in surface water and top-soil porewater, but increased sharply from 9 mm (1.5 mg/L) below SWI and reached up to 70 mg/L in 50 mm deep soils. Similar trends were observed for Mn, As, and P, which generally increased with depth. The similar vertical changes of Mn, As, P with Fe agree well with their tightly coupling in soils induced by dissimilatory Fe reducing bacteria (Arsic et al., 2018; Ma et al., 2017; Xu et al., 2017). At the 2–10 mm zone below SWI, a P pit was observed, which could be attributed to two reasons. First, unlike Fe, Mn, and As, P in surface water remained a relatively high concentration ($> 100 \mu\text{g/L}$), which indicated a constant P source existing in the surface water. This part of P is believed to have been released from dead algae degradation (Jarvie et al., 2008). Second, the dissolved P in surface water was trapped by the Fe oxides formed in SWI, where O_2 diffused from surface water reacted with ferrous ions from deep soil (Ajmal et al., 2018; Rietra et al., 2001).

The S behavior was distinct from Fe, Mn, P, and As (Fig. 2). The concentrations of S were high at flooded water and dropped with depth. Sulfur is believed to exist as S(VI) in oxic conditions (Wu et al., 2016), and biotic S(VI) reduction occurs when the redox potential in soils dropped to a highly reducing condition (after easily used electron acceptors were consumed, like O_2 , nitrate, Mn and Fe oxides) (Borch et al., 2010). The subsurface decrease of S is therefore presumably caused by S(VI) reducing bacteria in anoxic soils (Pester et al., 2012), which transformed mobile S(VI) to insoluble S(-II) minerals (e.g. FeS , FeS_2) (Wu et al., 2016).

To the best of our knowledge, there is no reported analytical method that can simultaneously measure major and trace elements in the redox gradient zone across SWI. Tradition-

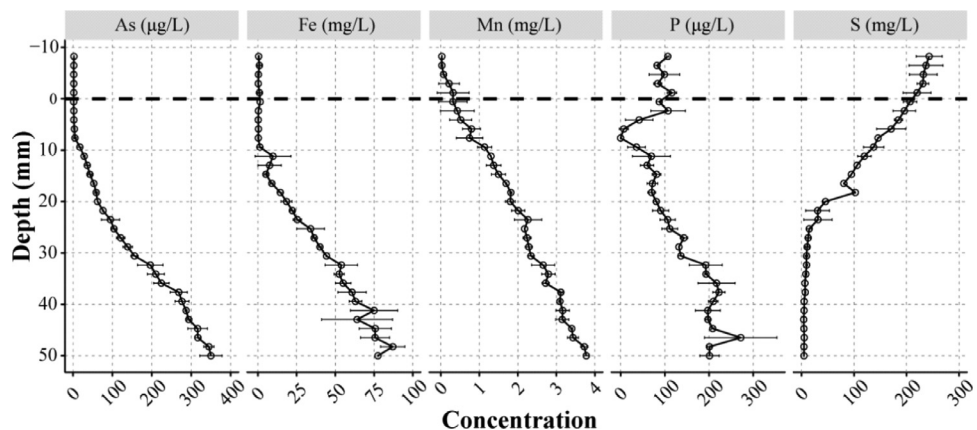


Fig. 2 – Mapping of As, Fe, Mn, P, and S profiles in Shaoguan (SG) paddy with ICP-MS.

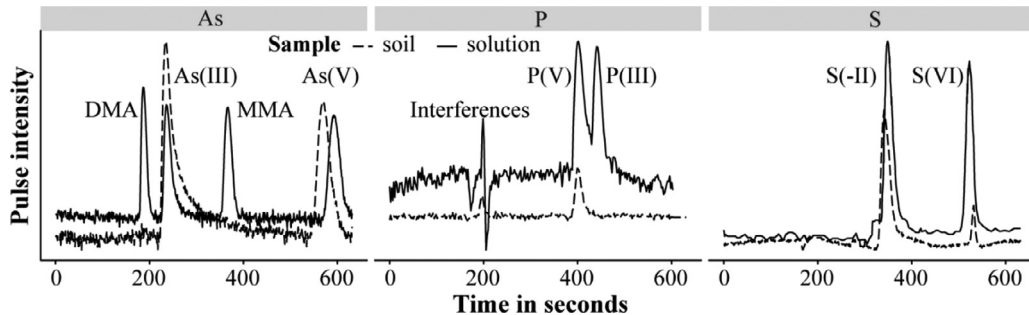


Fig. 3 – Arsenic (As), phosphorus (P), and sulfur (S) species detected by IC-ICP-MS. The samples include soil porewater and solution. The solution was prepared in neutral conditions (pH 7; 100 µg/L phosphite (P(III)), phosphate (P(V)), arsenite (As(III)), arsenate (As(V)), monomethylarsonic (MMA) and dimethylarsinic (DMA); 1 mg/L sulfide (S(-II)) and sulfate (S(VI))).

ally, a large volume of subsamples are required to measure Fe, Mn and P by colorimetric methods or ICP-OES (Arsic et al., 2018; Rietra et al., 2001; Serrat, 1998; Wang et al., 2019; Yi et al., 2019), S by IC (Keller-Lehmann et al., 2006), and most traces (e.g. As and antimony) by ICP-MS (Gustave et al., 2018a, 2019). It is obviously beneficial for studies on element biogeochemical cycles when all the elements can be measured in one injection. The ICP-MS based method dramatically reduces the time consumption for multi-element, thus significantly increases the measurement throughput. The method can also be coupled with other HR samplers, for example, DET and HR peeper.

2.5. As, P, and S species measurement with IC-ICP-MS

The As, P, and S species vary along SWI and determine their environmental fates. In this study, simultaneous detection of four As, two P, and two S species in solution and anoxic soil porewater was achieved with the NH_4HCO_3 as the mobile phase (Fig. 3). The retention times were 6.6, 7.5, 3.2, 3.9, 6.0, 10, 3.2, and 8.8 min for P(V), P(III), DMA, As(III), MMA, As(V), S(-II), and S(VI) respectively. The separation of four As species agrees

well with previous work using the same chromatographic conditions (Suzuki et al., 2009). The results also demonstrated NH_4HCO_3 mobile phase can be extended to measure P and S species. The determination coefficients for all the three elements are > 0.96 (Appendix A Fig. S8).

When applied to soil porewater, 2 As (As(III,V)), 1 P (P(V)), and 2 S (S(-II, VI)) species were detected (Fig. 3). Arsenite, P(V), and S(-II) (> 70%) represent the dominant As, P and S in soil porewater, respectively. These results agree well with previous reports from multiple soils when the HPLC-ICP-MS, IC or colorimetric methods were used (Chen et al., 2019; Han et al., 2018; Xu et al., 2017). Besides, a susceptible P peak was detected in both solution and porewater with a retention time of 200 s (Fig. 3). The retention time is very close to the column dead time for the IC-ICP-MS, which indicates this compound may be cations or small molecules. Among the P species found in environmental samples, phosphine was the only one with neutral in charge, but it is only found in highly reducing environments (Han et al., 2002), thus can be excluded. Therefore, we extrapolate the P peak at 200 s is likely an interference, such as $^{47}\text{Ti}^+$, which has the same mass-to-charge ratio of $^{47}\text{PO}^+$.

Table 1 – Separation of As, P and S species with IC-ICP-MS under different conditions.

Mobile phase	pH	Species measured	Tr. [§]	Ref.
HNO ₃	1.3 - 2.6	As(III, V), MMA, DMA	5	(Jackson and Bertsch, 2001)
C ₄ H ₁₀ O ₃ S [†] + C ₆ H ₁₄ O ₃ S [‡]	3.0	As(V), DMA	5	(Hirata and Toshimitsu, 2007)
NH ₄ NO ₃	5.1	P(V)	5	(Chen et al., 2009)
	7.0	S(IV, VI), thiosulfate	5	(Lin and Jiang, 2009)
	7.5	As(III, V), MMA, DMA, S(VI)	15	(Vriens et al., 2014)
NH ₄ NO ₃ + NH ₄ H ₂ PO ₄	7.2 + 8.2	As(III, V), MMA, DMA	15	(Paik et al., 2010)
NH ₄ HCO ₃	10	As(III, V), MMA, DMA	9	(Suzuki et al., 2009)
	10.7	P(III, V), S(-II, VI)	10	This study
K ₂ SO ₄	10.5	As(III, V), MMA, DMA	7	(Branch et al., 1989)
(NH ₄) ₂ CO ₃	11.2	As(V), P(V), S(VI)	4	(Divjak et al., 1999)
NaOH	> 12	As(III, V), MMA, DMA	8	(Jackson and Bertsch, 2001)
		S(-II, IV, VI)	8	(Divjak and Goessler, 1999)

[§] measurement throughput (min per sample).

[†] 1-butanesulfonic acid.

[‡] 1-hexanesulfonic acid; arsenite, As(III); arsenate, As(V); monomethylarsonic, MMA; dimethylarsinic, DMA; hypophosphite, P(I); phosphite, P(III); phosphate, P(V); sulfide, S(-II); sulfite, S(IV); sulfate, S(VI).

Many types of mobile phases were designed to measure the P, S, or As species (Table 1). Among the typical mobile phases, the carbonate-based mobile phase (NH₄HCO₃) is better than the others due to its capability to separate the common species of As, P, and S in 10 min. Other chemicals were not suited for various reasons. The P or S containing compounds, like K₂SO₄, 1-butanesulfonic acid, 1-hexanesulfonic acid and NH₄H₂PO₄, (Branch et al., 1989; Hirata and Toshimitsu, 2007; Paik et al., 2010) were first excluded because of their interferences with P and S measurement. Nitrate-based mobile phase, such as HNO₃ and NH₄NO₃, (Jackson and Bertsch, 2001; Paik et al., 2010) can be used to separate P and S species, but its elution strength is weaker than that of CO₃²⁻, which must be used in strong acid condition to shorten the retention time (Jackson and Bertsch, 2001), or in neutral condition with very long running time (Vriens et al., 2014). The acidic condition is not ideal for S(-II) detection, because it encourages gaseous H₂S formation. The alkali hydroxyl-based mobile phase is widely used to As and S species measurement by IC-ICP-MS (Divjak and Goessler, 1999; Jackson and Bertsch, 2001). However, the hydroxyl-based mobile phase often contains alkali metal cations, like sodium, which can clog the plasma torch, sampling corn, or skimmer corn by the inorganic salts deposition. Thus, NH₄HCO₃ is the best choice to develop a mobile phase for simultaneously separating P, S, and As species.

The NH₄HCO₃ mobile phase pH (10.7) is appropriate to form P, S, and As species of different charges (Divjak and Goessler, 1999; McDowell et al., 2004; Reid et al., 2020). However, the alkali condition may cause Fe oxides precipitation when the mobile phase mixed with the high Fe porewater. The precipitates could bind with the anions, and potentially interfere with the testing and cause clog in the analytical column. Thus, EDTA was pre-added into samples before sample injection to the IC. EDTA could mitigate the precipitation of metal ions within a wide range of pH (Almkvist et al., 2013; Gallagher et al., 2001; Samanta and Clifford, 2006). With EDTA

addition, no metal oxides precipitation was observed during IC-ICP-MS measurement.

2.6. Profiling of P, S and As species across SWI

The optimized IC-ICP-MS method was further verified with soil porewater collected by SWI profilers. The vertical changes of As(III), As(V), P(V), S(-II) and S(IV) are depicted in Fig. 4. Among the species, As(III), As(V), P(V) and S(-II) were low in top layers, and increased gradually from 7.9, 0.70, 60 µg/L and 1.6 mg/L at ~ 13 mm below SWI to over 200, 50, 200 µg/L and 15 mg/L in deep soils respectively. The S(VI) change was consistent with the total S, which decreased along the soil depth (Fig. 4). The As, P and S trends agree with their fates in flooded soils, and the results revealed by other methods (Arsic et al., 2018; Han et al., 2018; Mcadams et al., 2016; Robertson et al., 2008).

According to the element profiles, we noticed that there was an overlap between dissolved Fe and S(-II) in pretty high concentrations at > 15 mm below SWI (Figs. 2 and 4). Ferrous ions are the main form of dissolved Fe in reducing condition, and not supposed to co-exist with S(-II) in aqueous phase in theory because they form insoluble FeS (Rickard, 2006). However, the co-existence of ferrous ions and S(-II) were frequently reported in many field samples (Pagès et al., 2011; Robertson et al., 2008, 2009) and we speculate that the ferrous ions may be chelated with dissolved organic matters and stabilized in aqueous phase.

Although the redox-sensitive elements speciation has received much attention, most analytical methods for those species were developed for single element only (Divjak and Goessler, 1999; Han et al., 2018; Jackson and Bertsch, 2001). In comparison with those methods, the optimized method in the current study has higher measurement throughput, which can simultaneously measure As, P and S species within 10 min

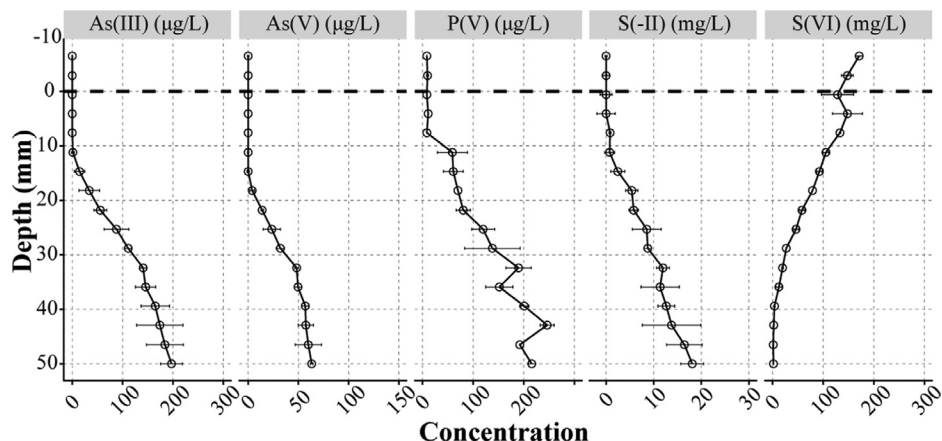


Fig. 4 – Profiles of P, S and As species in SG paddy measured by SWI profiler and NH_4HCO_3 eluent.

in a single run. The method is well suited for coupling with HR samplers to map multi-species profiles across SWI.

3. Conclusions

Simultaneous measurement of multi-element (Fe, Mn, As, P, S) and multi-species (As(III), As(V), MMA, DMA, P(III), P(V), S(-II) and S(VI)), in volume-limited samples ($\sim 100 \mu\text{L}$ level), was achieved with the ICP-MS and IC-ICP-MS analysis. The method demonstrated both high sensitivity ($\mu\text{g/L}$ level) and high throughput. Combining the optimized analytical methods and a HR porewater sampler (i.e. IPI), we successfully measured the mm-scale co-distributions of multi-element (Fe, Mn, As, P and S) and multi-species (As(III), As(V), P(V), S(-II) and S(VI)) along SWI. With rapid measurement of multiple parameters from limited samples, the optimized analytical methods enable researchers to measure aqueous chemistry (including pure solution, surface water, porewater and groundwater) at high throughput. Moreover, the optimized analytical methods are very well suited for limited samples analysis in HR samplers (e.g. IPI, DET and peeper). The combination of the method and HR samplers can provide as much as possible aqueous parameters, thus facilitate studies of elements cycling in micro interfaces (e.g. SWI) of soils, sediments and other aqueous environments.

Acknowledgments

This work was supported by the National Science Foundation of China (Nos. 41977320, 41571305), Key Programme Special Fund of XJTLU (No. KSF-A-20). The authors acknowledge the kind help of Fuyuan Liu for the 3D printing model design. The authors also acknowledge the kind help of Yi-Li Cheng, Xiao Zhou, Xiao-Yan Zhang, and Liang-Ping Long for their support in instrumental analysis.

Appendix A. Supplementary data

Supplementary material associated with this article can be found, in the online version, at doi:[10.1016/j.jes.2020.09.017](https://doi.org/10.1016/j.jes.2020.09.017).

REFERENCES

- Ajmal, Z., Muhammed, A., Usman, M., Kizito, S., Lu, J., Dong, R., et al., 2018. Phosphate removal from aqueous solution using iron oxides: adsorption, desorption and regeneration characteristics. *J. Colloid Interface Sci.* 528, 145–155.
- Almkvist, G., Hocker, E., Sahlstedt, M., Museums, S.M., 2013. Iron Removal From Waterlogged Wood. Swedish University of Agricultural Sciences. SLU Repro, Uppsala.
- Arsic, M., Teasdale, P.R., Welsh, D.T., Johnston, S.G., Burton, E.D., Hockmann, K., et al., 2018. Diffusive gradients in thin films (DGT) reveals antimony and arsenic mobility differs in a contaminated wetland sediment during an oxic-anoxic transition. *Environ. Sci. Technol.* 52, 1118–1127.
- Bennett, W.W., Teasdale, P.R., Panther, J.G., Welsh, D.T., Zhao, H., Jolley, D.F., 2012a. Investigating arsenic speciation and mobilization in sediments with DGT and DET: a mesocosm evaluation of oxic-anoxic transitions. *Environ. Sci. Technol.* 46, 3981–3989.
- Bennett, W.W., Teasdale, P.R., Welsh, D.T., Panther, J.G., Jolley, D.F., 2012b. Optimization of colorimetric DET technique for the in situ, two-dimensional measurement of iron (II) distributions in sediment porewaters. *Talanta* 88, 490–495.
- Borch, T., Kretzschmar, R., Kappler, A., Cappellen, P.V., Gindervogel, M., Voegelin, A., et al., 2010. Biogeochemical redox processes and their impact on contaminant dynamics. *Environ. Sci. Technol.* 44, 15–23.
- Bottrell, S.H., Mortimer, R.J., Spence, M., Krom, M.D., Clark, J.M., Chapman, P.J., 2007. Insights into redox cycling of sulfur and iron in peatlands using high-resolution diffusive equilibrium thin film (DET) gel probe sampling. *Chem. Geol.* 244, 409–420.
- Branch, S., Bancroft, K., Ebdon, L., O'Neill, P., 1989. The determination of arsenic species by coupled high-performance liquid chromatography-atomic spectrometry. *Anal. Proc.* 26, 73–75.
- Braunschweig, J., Bosch, J., Heister, K., Kuebeck, C., Meckenstock, R.U., 2012. Reevaluation of colorimetric iron

- determination methods commonly used in geomicrobiology. *J. Microbiol. Methods* 89, 41–48.
- Chen, C., Li, L., Huang, K., Zhang, J., Xie, W.Y., Lu, Y., et al., 2019. Sulfate-reducing bacteria and methanogens are involved in arsenic methylation and demethylation in paddy soils. *ISME J.* 13, 2523–2535.
- Chen, Z., He, W., Beer, M., Megharaj, M., Naidu, R., 2009. Speciation of glyphosate, phosphate and aminomethylphosphonic acid in soil extracts by ion chromatography with inductively coupled plasma mass spectrometry with an octopole reaction system. *Talanta* 78, 852–856.
- Cheng, G., He, M., Peng, H., Hu, B., 2012. Dithizone modified magnetic nanoparticles for fast and selective solid phase extraction of trace elements in environmental and biological samples prior to their determination by ICP-OES. *Talanta* 88, 507–515.
- Cotta, A.J.B., Enzweiler, J., 2009. Quantification of major and trace elements in water samples by ICP-MS and collision cell to attenuate Ar and Cl-based polyatomic ions. *J. Anal. Atom. Spectrom.* 24, 1406–1413.
- Davison, W., Zhang, H., 1994. In situ speciation measurements of trace components in natural waters using thin-film gels. *Nature* 367, 546.
- Di, X., Wei, W., Shiming, D., Qin, S., Chaosheng, Z., 2012. A high-resolution dialysis technique for rapid determination of dissolved reactive phosphate and ferrous iron in pore water of sediments. *Sci. Total Environ.* 421–422, 245–252.
- Ding, S., Wang, Y., Wang, D., Li, Y.Y., Gong, M., Zhang, C., 2016. In situ, high-resolution evidence for iron-coupled mobilization of phosphorus in sediments. *Sci. Rep.* 6, 24341.
- Divjak, B., Goessler, W., 1999. Ion chromatographic separation of sulfur-containing inorganic anions with an ICP-MS as element-specific detector. *J. Chromatogr. A* 844, 161–169.
- Divjak, B., Novič, M., Goessler, W., 1999. Determination of bromide, bromate and other anions with ion chromatography and an inductively coupled plasma mass spectrometer as element-specific detector. *J. Chromatogr. A* 862, 39–47.
- Dočekalová, H., Clarisse, O., Salomon, S., Wartel, M., 2002. Use of constrained DET probe for a high-resolution determination of metals and anions distribution in the sediment pore water. *Talanta* 57, 145–155.
- Fang, W., Williams, P.N., Fang, X., Amoah-Antwi, C., Yin, D., Li, G., et al., 2018. Field-scale heterogeneity and geochemical regulation of arsenic, iron, lead, and sulphur bioavailability in paddy soil. *Environ. Sci. Technol.* 52, 12098–12107.
- Frenzel, P., Rothfuss, F., Conrad, R., 1992. Oxygen profiles and methane turnover in a flooded rice microcosm. *Biol. Fert. Soils* 14, 84–89.
- Gallagher, P.A., Schwegel, C.A., Wei, X., Creed, J.T., 2001. Speciation and preservation of inorganic arsenic in drinking water sources using EDTA with IC separation and ICP-MS detection. *J. Environ. Monit.* 3, 371–376.
- Gao, L., Gao, B., Zhou, H., Xu, D., Wang, Q., Yin, S., 2016. Assessing the remobilization of antimony in sediments by DGT: a case study in a tributary of the Three Gorges reservoir. *Environ. Pollut.* 214, 600–607.
- Gao, Y., Leermakers, M., Elskens, M., Billon, G., Ouddane, B., Fischer, J.-C., et al., 2007. High resolution profiles of thallium, manganese and iron assessed by DET and DGT techniques in riverine sediment pore waters. *Sci. Total Environ.* 373, 526–533.
- Gao, Y., Leermakers, M., Gabelle, C., Divis, P., Billon, G., Ouddane, B., et al., 2006. High-resolution profiles of trace metals in the pore waters of riverine sediment assessed by DET and DGT. *Sci. Total Environ.* 362, 266–277.
- Guan, D.X., Williams, P.N., Luo, J., Zheng, J.L., Xu, H.C., Cai, C., et al., 2015. Novel precipitated zirconia-based DGT technique for high-resolution imaging of oxyanions in waters and sediments. *Environ. Sci. Technol.* 49, 3653–3661.
- Gustave, W., Yuan, Z.F., Sekar, R., Chang, H.C., Zhang, J., Wells, M., et al., 2018a. Arsenic mitigation in paddy soils by using microbial fuel cells. *Environ. Pollut.* 238, 647–655.
- Gustave, W., Yuan, Z.F., Sekar, R., Ren, Y.X., Chang, H.C., Liu, J.Y., et al., 2018b. The change in biotic and abiotic soil components influenced by paddy soil microbial fuel cells loaded with various resistances. *J. Soil. Sediment.* 19, 106–115.
- Gustave, W., Yuan, Z.F., Sekar, R., Ren, Y.X., Liu, J.Y., Zhang, J., et al., 2019. Soil organic matter amount determines the behavior of iron and arsenic in paddy soil with microbial fuel cells. *Chemosphere* 237, 124459.
- Han, C., Williams, P.N., Ren, J., Wang, Z., Fang, X., Xu, D., et al., 2018. In situ sampling and speciation method for measuring dissolved phosphite at ultratrace concentrations in the natural environment. *Water Res.* 137, 281–289.
- Han, S., Zhuang, Y., Zhang, H., Wang, Z., Yang, J., 2002. Phosphine and methane generation by the addition of organic compounds containing carbon–phosphorus bonds into incubated soil. *Chemosphere* 49, 651–657.
- Hatat-Fraile, M., Barbeau, B., 2019. Performance of colorimetric methods for the analysis of low levels of manganese in water. *Talanta* 194, 786–794.
- Hilbig, H., Huber, M., Gmell, A., Heinz, D., 2017. Determination of heavy metals in a highly porous sorptive filter material of road runoff treatment systems with LA-ICP-MS. *Water Air Soil Pollut.* 228, 331.
- Hirata, S., Toshimitsu, H., 2007. Determination of arsenic species and arsenosugars in marine samples by HPLC-ICP-MS. *Appl. Organomet. Chem.* 21, 447–454.
- Huo, S., Zhang, J., Yeager, K.M., Xi, B., Qin, Y., He, Z., et al., 2015. Mobility and sulfidization of heavy metals in sediments of a shallow eutrophic lake, Lake Taihu, China. *J. Environ. Sci.* 31, 1–11.
- Jackson, B.P., Bertsch, P.M., 2001. Determination of arsenic speciation in poultry wastes by IC-ICP-MS. *Environ. Sci. Technol.* 35, 4868–4873.
- Jarvie, H.P., Mortimer, R.J., Palmer-Felgate, E.J., Quinton, K.S., Harman, S.A., Carbo, P., 2008. Measurement of soluble reactive phosphorus concentration profiles and fluxes in river-bed sediments using DET gel probes. *J. Hydrol.* 350, 261–273.
- Jones, M.E., Nico, P.S., Ying, S., Regier, T., Thieme, J., Keiluweit, M., 2018. Manganese-driven carbon oxidation at oxic–anoxic interfaces. *Environ. Sci. Technol.* 52, 12349–12357.
- Keller-Lehmann, B., Corrie, S., Ravn, R., Yuan, Z., Keller, J., 2006. Preservation and simultaneous analysis of relevant soluble sulfur species in sewage samples. In: Proceedings of the Second International IWA Conference on Sewer Operation and Maintenance, 26, p. 28.
- Laskov, C., Herzog, C., Lewandowski, J., Hupfer, M., 2007. Miniaturized photometrical methods for the rapid analysis of phosphate, ammonium, ferrous iron, and sulfate in pore water of freshwater sediments. *Limnol. Oceanogr. Methods* 5, 63–71.
- Lin, L.-Y., Jiang, S.-J., 2009. Determination of sulfur compounds in water samples by ion chromatography dynamic reaction cell inductively coupled plasma mass spectrometry. *J. Chin. Chem. Soc.* 56, 967–973.
- Lumbaque, E.C., da Silva, B.A., Böck, F.C., Helfer, G.A., Ferrão, M.F., Sirtori, C., 2019. Total dissolved iron and hydrogen peroxide determination using the PhotoMetrixPRO application: a portable colorimetric analysis tool for controlling important conditions in the solar photo-Fenton process. *J. Hazard. Mater.* 378, 120740.
- Ma, W.W., Zhu, M.X., Yang, G.P., Li, T., 2017. In situ, high-resolution DGT measurements of dissolved sulfide, iron and phosphorus in sediments of the East China Sea: insights into phosphorus mobilization and microbial iron reduction. *Mar. Pollut. Bull.* 124, 400–410.

- Mcadams, B.C., Adams, R.M., Arnold, W.A., Chin, Y.P., 2016. Novel insights into the distribution of reduced sulfur species in prairie pothole wetland pore waters provided by bismuth film electrodes. *Environ. Sci. Technol. Lett.* 3, 104–109.
- McDowell, M.M., Ivey, M.M., Lee, M.E., Firpo, V.V., Salmassi, T.M., Khachikian, C.S., et al., 2004. Detection of hypophosphite, phosphite, and orthophosphate in natural geothermal water by ion chromatography. *J. Chromatogr. A* 1039, 105–111.
- Miranda, J.L., Mesquita, R.B., Nunes, A., Rangel, M., Rangel, A.O., 2016. Iron speciation in natural waters by sequential injection analysis with a hexadentate 3-hydroxy-4-pyridinone chelator as chromogenic agent. *Talanta* 148, 633–640.
- Monbet, P., McKelvie, I.D., Worsfold, P.J., 2008. Combined gel probes for the *in situ* determination of dissolved reactive phosphorus in porewaters and characterization of sediment reactivity. *Environ. Sci. Technol.* 42, 5112–5117.
- Morton, S.C., Glindemann, D., Wang, X., Niu, X., Edwards, M., 2005. Analysis of reduced phosphorus in samples of environmental interest. *Environ. Sci. Technol.* 39, 4369–4376.
- Motelica-Heino, M., Naylor, C., Zhang, H., Davison, W., 2003. Simultaneous release of metals and sulfide in lacustrine sediment. *Environ. Sci. Technol.* 37, 4374–4381.
- Pages, A., Teasdale, P.R., Robertson, D., Bennett, W.W., Schäfer, J., Welsh, D.T., 2011. Representative measurement of two-dimensional reactive phosphate distributions and co-distributed iron (II) and sulfide in seagrass sediment porewaters. *Chemosphere* 85, 1256–1261.
- Paik, M.K., Kim, M.J., Kim, W.I., Yoo, J.H., Park, B.J., Im, G.J., et al., 2010. Determination of arsenic species in polished rice using a methanol-water digestion method. *J. Korean Soc. Appl. Biol. Chem.* 53, 634–638.
- Peng, C., Bryce, C., Sundman, A., Kappler, A., 2019. Cryptic cycling of complexes containing Fe (III) and organic matter by phototrophic Fe (II)-oxidizing bacteria. *Appl. Environ. Microbiol.* 85 e02826–02818.
- Persson, D.P., Hansen, T.H., Laursen, K.H., Schjoerring, J.K., Husted, S., 2009. Simultaneous iron, zinc, sulfur and phosphorus speciation analysis of barley grain tissues using SEC-ICP-MS and IP-ICP-MS. *Metallomics* 1, 418–426.
- Pester, M., Knorr, K.H., Friedrich, M.W., Wagner, M., Loy, A., 2012. Sulfate-reducing microorganisms in wetlands—fameless actors in carbon cycling and climate change. *Front. Microbiol.* 3, 72.
- Pi, K., Wang, Y., Postma, D., Teng, M., Su, C., Xie, X., 2018. Vertical variability of arsenic concentrations under the control of iron-sulfur-arsenic interactions in reducing aquifer systems. *J. Hydrol.* 561, 200–210.
- Ratering, S., Schnell, S., 2001. Nitrate-dependent iron (II) oxidation in paddy soil. *Environ. Microbiol.* 3, 100–109.
- Reid, M.S., Hoy, K.S., Schofield, J.R.M., Uppal, J.S., Lin, Y., Lu, X., et al., 2020. Arsenic speciation analysis: a review with an emphasis on chromatographic separations. *Trend. Anal. Chem.* 123, 115770.
- Reynolds, B., Stevens, P., Hughes, S., Brittain, S., 2004. Comparison of field techniques for sampling soil solution in an upland peatland. *Soil Use Manag.* 20, 454–456.
- Rickard, D., 2006. The solubility of FeS. *Geochim. Cosmochim. Acta* 70, 5779–5789.
- Rietra, R.P.J.J., Hiemstra, T., Van Riemsdijk, W.H., 2001. Interaction between calcium and phosphate adsorption on goethite. *Environ. Sci. Technol.* 35, 3369–3374.
- Robertson, D., Teasdale, P.R., Welsh, D.T., 2008. A novel gel-based technique for the high resolution, two-dimensional determination of iron (II) and sulfide in sediment. *Limnol. Oceanogr. Methods* 6, 502–512.
- Robertson, D., Welsh, D.T., Teasdale, P.R., 2009. Investigating biogenic heterogeneity in coastal sediments with two-dimensional measurements of iron (II) and sulfide. *Environ. Chem.* 6, 60–69.
- Samanta, G., Clifford, D.A., 2006. Preservation and field speciation of inorganic arsenic species in groundwater. *Water Qual. Res. J. Can.* 41, 107–116.
- Seeberg-Elverfeldt, J., Schlüter, M., Feseker, T., Kölling, M., 2005. Rhizon sampling of porewaters near the sediment-water interface of aquatic systems. *Limnol. Oceanogr. Methods* 3, 361–371.
- Serrat, F.B., 1998. 3, 3', 5, 5'-Tetramethylbenzidine for the colorimetric determination of manganese in water. *Microchim. Acta* 129, 77–80.
- Sun, Q., Ding, S., Zhang, L., Chen, M., Zhang, C., 2017. A millimeter-scale observation of the competitive effect of phosphate on promotion of arsenic mobilization in sediments. *Chemosphere* 180, 285.
- Suzuki, Y., Shimoda, Y., Endo, Y., Hata, A., Yamanaka, K., Endo, G., 2009. Rapid and effective speciation analysis of arsenic compounds in human urine using anion-exchange columns in HPLC-ICP-MS. *J. Occup. Health* 51, 380–385.
- Tanner, S.D., Baranov, V.I., 1999. A dynamic reaction cell for inductively coupled plasma mass spectrometry (ICP-DRC-MS). II. Reduction of interferences produced within the cell. *J. Am. Soc. Mass Spectr.* 10, 1083–1094.
- Vriens, B., Ammann, A.A., Hagendorfer, H., Lenz, M., Berg, M., Winkel, L.H.E., 2014. Quantification of methylated selenium, sulfur, and arsenic in the environment. *PLoS ONE* 9 e102906–e102906.
- Wang, M., Tang, Z., Chen, X.P., Wang, X., Zhou, W.X., Tang, Z., et al., 2019. Water management impacts the soil microbial communities and total arsenic and methylated arsenicals in rice grains. *Environ. Pollut.* 247, 736–744.
- Wen, S., Wu, T., Yang, J., Jiang, X., Zhong, J., 2019. Spatio-temporal variation in nutrient profiles and exchange fluxes at the sediment-water interface in Yuqiao reservoir, China. *Int. J. Environ. Res. Public Health* 16, 3071.
- Williams, P.N., Santner, J., Larsen, M., Lehto, N.J., Oburger, E., Wenzel, W., et al., 2014. Localized flux maxima of arsenic, lead, and iron around root apices in flooded lowland rice. *Environ. Sci. Technol.* 48, 8498–8506.
- Wu, Z., Ren, D., Zhou, H., Hang, G., Li, J., 2016. Sulfate reduction and formation of iron sulfide minerals in nearshore sediments from Qi'ao Island, Pearl River Estuary, Southern China. *Quatern. Int.* 452, 137–147.
- Xu, D., Wu, W., Ding, S., Sun, Q., Zhang, C., 2012. A high-resolution dialysis technique for rapid determination of dissolved reactive phosphate and ferrous iron in pore water of sediments. *Sci. Total Environ.* 421, 245–252.
- Xu, X., Chen, C., Wang, P., Kretzschmar, R., Zhao, F.J., 2017. Control of arsenic mobilization in paddy soils by manganese and iron oxides. *Environ. Pollut.* 231, 37–47.
- Yi, X.Y., Yang, Y.P., Yuan, H.Y., Chen, Z., Duan, G.L., Zhu, Y.G., 2019. Coupling metabolisms of arsenic and iron with humic substances through microorganisms in paddy soil. *J. Hazard. Mater.* 373, 591–599.
- Yin, D.X., Fang, W., Guan, D.X., Williams, P.N., Moreno Jimenez, E., Gao, Y., et al., 2020. Localized intensification of arsenic release within the emergent rice rhizosphere. *Environ. Sci. Technol.* 54, 3138–3147.
- Yuan, Z.F., Gustave, W., Bridge, J., Liang, Y., Sekar, R., Boyle, J., et al., 2019. Tracing the dynamic changes of element profiles by novel soil porewater samplers with ultralow disturbance to soil-water interface. *Environ. Sci. Technol.* 53, 5124–5132.
- Zhai, H., Wang, L., Hövelmann, J., Qin, L., Zhang, W., Putnis, C.V., 2018. Humic acids limit the precipitation of cadmium and arsenate at the Brushite– Fluid interface. *Environ. Sci. Technol.* 53, 194–202.